Journal of Physics: Condensed Matter

PAPER

Hydrogen adsorption on nitrogen and boron doped graphene

To cite this article: Michele Pizzochero *et al* 2015 *J. Phys.: Condens. Matter* **27** 425502

IOP Publishing

Journal of Physics: Condensed Matter

J. Phys.: Condens. Matter **27** (2015) 425502 (11pp)

doi:10.1088/0953-8984/27/42/425502

Hydrogen adsorption on nitrogen and boron doped graphene

Michele Pizzochero[1], **Ortwin Leenaerts**[3], **Bart Partoens**[3], **Rocco Martinazzo**[1,2] **and François M Peeters**[3]

[1] Dipartimento di Chimica, Università degli Studi di Milano, via Golgi 19, 20133 Milan, Italy
[2] CNR-ISTM, Istituto di Scienze e Tecnologie Molecolari, via Golgi 19, 20133 Milan, Italy
[3] Departement Fysica, Universiteit Antwerpen, Groenenborgerlaan 171, B- 2020 Antwerpen, Belgium

E-mail: ortwin.leenaerts@uantwerpen.be and rocco.martinazzo@unimi.it

Received 12 June 2015, revised 23 August 2015
Accepted for publication 7 September 2015
Published 6 October 2015

Abstract

Hydrogen adsorption on boron and nitrogen doped graphene is investigated in detail by means of first-principles calculations. A comprehensive study is performed of the structural, electronic, and magnetic properties of chemisorbed hydrogen atoms and atom pairs near the dopant sites. The main effect of the substitutional atoms is charge doping which is found to greatly affect the adsorption process by increasing the binding energy at the sites closest to the substitutional species. It is also found that doping does not induce magnetism despite the odd number of electrons per atom introduced by the foreign species, and that it quenches the paramagnetic response of chemisorbed H atoms on graphene. Overall, the effects are similar for B and N doping, with only minor differences in the adsorption energetics due to different sizes of the dopant atoms and the accompanying lattice distortions.

Keywords: doping, hydrogenation, first-principles

(Some figures may appear in colour only in the online journal)

1. Introduction

Since the discovery of graphene in 2004 [1, 2], a large body of experimental and theoretical works addressed the possibility of controlling and changing the properties of this interesting material. A straightforward way to accomplish this is through functionalization of the graphene surface. Graphene is only one atom thick so it is completely exposed to its environment. Atoms and molecules can readily adsorb to its surface and alter the physical behavior by disturbing the π-electron network that is so typical for graphene. In this way, graphene can be transformed from a semimetal into a semiconductor, with a band gap width that can be tuned by controlling the level of functionalization. There are several different adsorbates that can be used to functionalize graphene such as gas molecules and radicals, but the most broadly studied adsorbate is undoubtedly hydrogen [3–5]. There are many reasons for this: hydrogen is a widely available element and it is an ideal partner for carbon atoms to make strong covalent bonds with. Furthermore, the high chemical stability and large surface-to-volume ratios of several carbon allotropes—e.g. activated carbons [6], carbon nanotubes [7], graphite nanofibers [8], and other graphene-based nanomaterials [9]—make them ideal as hydrogen storage materials. In general, hydrogen atoms effectively act as p_z vacancies in the graphene lattice, since they form strong chemical bonds with a single C atom each and essentially remove p_z orbitals from the π electron cloud, thereby introducing 'midgap' states in the substrate electronic structure. As a consequence, they form strong, short-ranged (resonant) scatterers for charge carriers limiting their mobility at zero and finite carrier densities [10], leave a quasi-localized spin-half magnetic moment in their neighborhood and bias chemical reactivity towards specific lattice positions [11].

Another way to functionalize graphene is through substitutional doping. Some C atoms in the graphene layer are substituted for other atoms such as boron and nitrogen. This kind of substitutional doping has been achieved in experiments for B and N atoms [12–14]. The foreign atoms have different sizes and can induce some strain or buckling into the system, but the most important consequence of substitutional doping is the possibility of charge doping. The dopant atoms usually have a different number of valence electrons and therefore add electrons to or remove electrons from graphene. Since pure graphene has a vanishing density of charge carriers at the Dirac point, this has important consequences for the electronic properties. In addition to charge doping, substitutional doping causes some carbon-based materials to become superconductors. This has been experimentally demonstrated for B-doped diamond [15] and was also predicted for B-doped hydrogenated graphene (graphane) [16].

In this work, we examine in detail the influence that dopant atoms have on the adsorption properties of graphene, focusing on boron and nitrogen doped graphene. Previous theoretical work on H adsorption on B-doped [17–19] and N-doped [20] graphene has already appeared in the literature, but information remains rather scattered and incomplete. A well-rounded perspective of the topic is still missing, and is highly desirable to solve unsettled issues concerning the magnetic properties of doped graphene and its chemistry. We provide here this picture by consistently including spin-polarization in the calculations, and by analyzing in detail the charge transferred to the lattice, the distortion which is necessary to accommodate the doping species, and the fate of the universal impurity ‘midgap’ states introduced upon hydrogen adsorption. We thus give a detailed explanation of the influence of both N- and B-doping on H chemisorption and uncover the underlying physical causes of the observed effects.

Our work is organized as follows: first we study the structural, electronic, and magnetic properties of B- and N-doped graphene, also examining the influence of the size of the supercell that is used in the simulations. Next, we investigate the adsorption of a single hydrogen atom at the dopant site and in the neighborhood of the substitutional foreign atom. We compare this ‘chemical’ doping with physical doping, whereby charges are injected by electrostatic gating. Finally, we investigate hydrogen pair adsorption in the neighborhood of the foreign atom, and provide detailed information about the stability of the chemisorbed H pairs and their magnetic properties.

2. Computational details

All our first-principles calculations were performed within the pseudopotential density functional theory formalism [21, 22] as implemented in the SIESTA code [23]. The generalized gradient approximation of Perdew, Burke, and Ernzerhof (GGA-PBE) was used for the exchange-correlation functional [24] and spin polarization was always included in the calculations. Valence electrons were described by a double-ζ basis with polarization (DZP) and their interaction with the core electrons was represented by norm-conserving pseudopotentials [25]. A mesh cutoff of 500 Ry was used for the charge density and found large enough to remove any egg-box effect from the structural relaxations. Integrations over the Brillouin zone were performed with the equivalent of a $36 \times 36 \times 1$ Monkhorst-Pack k-mesh [26] over a graphene unit cell in the geometry optimization runs, and increased to $150 \times 150 \times 1$ when computing the density of states. Our systems consisted of 4×4 or 6×6 graphene supercells with a vacuum layer of 15 Å between periodic images to reduce artificial interlayer interactions. Additionally, for a few selected cases, we also made use of a much larger supercell (a rectangular 5×12 supercell containing 240 atoms) to accommodate long-range effects that do not adequately fit in the above supercells; the choice of a rectangular supercell further removes any oddity arising from the high symmetry of the ensuing superlattices. In this case a $16 \times 12 \times 1$ k-mesh was adopted. Atomic positions were fully relaxed until the forces were lower than 0.01 eV Å^{-1}.

Table 1. The bond length between the foreign atom and the nearest-neighbor C atom, d_{CX}, the formation energy, and the magnetic moment in B- and N-doped graphene.

	B		N	
	4×4	6×6	4×4	6×6
d_{CX}	1.486	1.489	1.412	1.410
E_{form}	3.729	3.675	1.655	1.638
μ	0.0	0.0	0.0	0.0

Note: Distances are given in Å, energies in eV, and magnetic moments in μ_B.

We define the chemisorption energy of a hydrogen atom as $E_{chem} = E_{host+H} - E_{host} - E_H$, where E_{host} is the energy of the host system and E_H is the energy of an isolated H atom. The host is either B- or N- doped graphene for single-H adsorption, and is hydrogenated doped graphene for sequential adsorption to form dimers on the surface. Similarly, the doping ‘formation’ energy is defined as $E_{form} = E_{X+graph} - E_{graph} - E_X + E_C$, where $E_{X+graph}$ and E_{graph} are the energies of doped and undoped graphene, respectively, and E_X and E_C are the non-spin-polarized energies of the isolated dopant and a carbon atom. Notice that the latter are *not* the conventional thermodynamic formation energies (defined with respect to the constituent elements in their standard states), but rather they are operative formation energies which describe replacement of a lattice C atom from a gas-phase B or N atom. Finally, we define the reconstruction energy E_{surf} in the hydrogen adsorption process as the difference in energy between the adsorbate-free reconstructed surface and its relaxed (planar) geometry. In this way, we quantify the important contribution of energy going into the lattice because of the $sp^2 \rightarrow sp^3$ rehybridization which is always needed for a carbon atom to form a C-H bond.

3. Results

3.1. B- and N-doped graphene

Before investigating H adsorption on graphene with single atom substitutions, we first examine the structural and electronic properties of B and N-doped graphene. We used two different supercells, namely a 4×4 and a 6×6 supercell, to investigate the influence of the system size; the results of these preliminary calculations are summarized in table 1.

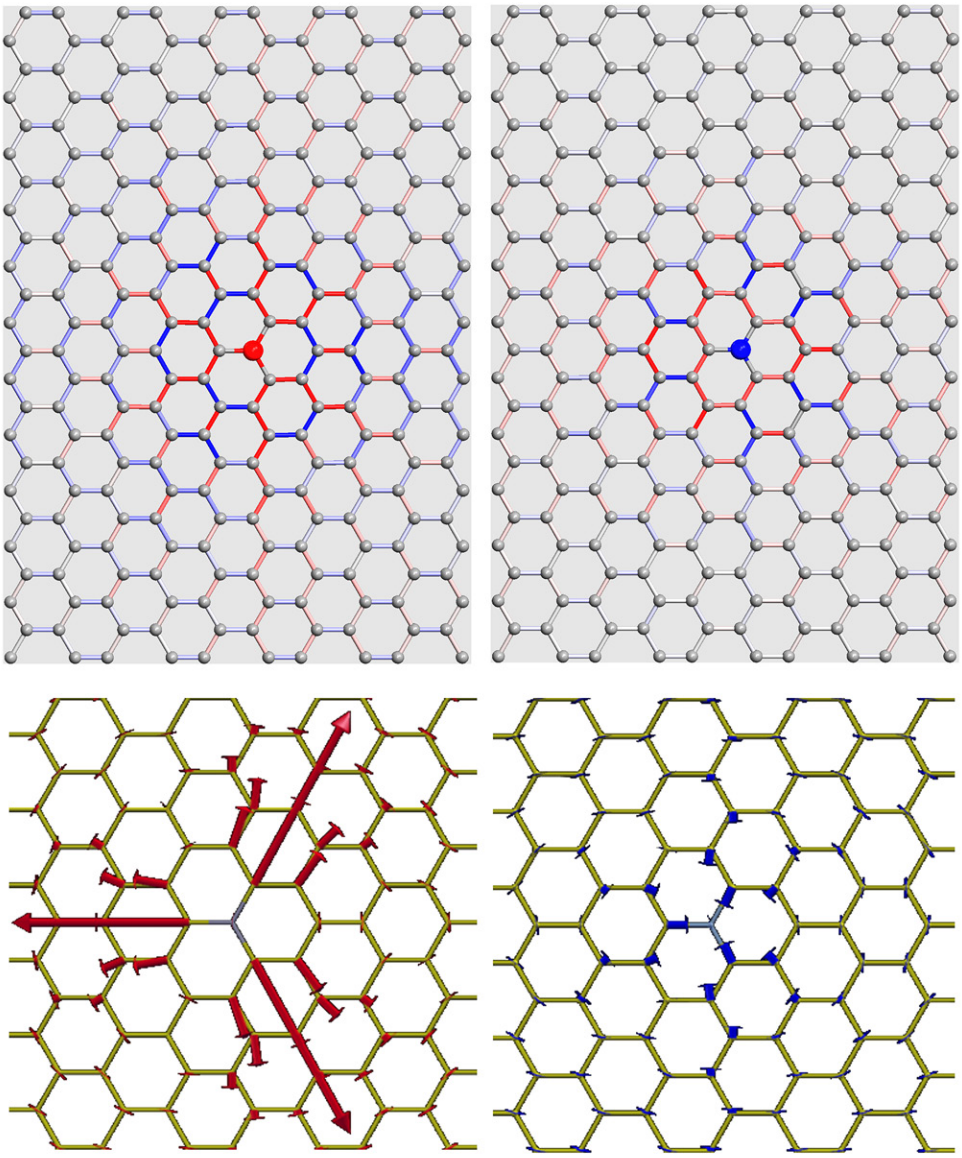

Figure 1. Top panels: Dopant-induced strain fields for boron (left panel) and nitrogen (right panel) substitution in a 5×12 supercell. Short bonds are in red and long bonds in blue, with colors varying from white to blue/red for bond lengths ranging from the equilibrium C-C distance in graphene to $\pm 0.25\%$. Bottom panels: unrelaxed, doped graphene lattices (B- and N- in the left and right panel, respectively) with vectors proportional to the displacements found in the corresponding relaxed structures.

Our findings agree well with previous works [27–30] and are very similar for the two different supercells. Graphene retains a planar structure after B- and N-doping, but there appears to be some in-plane strain induced by the B atom. The interatomic bond length changes from 1.41 Å for C-C bonds to 1.49 Å for C-B bonds. The C-N bonds, on the other hand, are only slightly shorter than the C-C bonds and almost do not perturb the graphene structure. Figure 1 shows the structural distortion induced by the foreign atom in the lattice, as obtained by calculations using the rectangular 5×12 supercell. It can be clearly observed that the nitrogen atom induces a milder strain in the graphene sheet than boron. This is mainly a consequence of the size of the substitutional atoms, since the covalent radius of nitrogen (71 pm) is very close to that of carbon (73 pm), and significantly smaller than that of boron (84 pm). The different structural distortion caused by the B and N substitution has a strong effect on the stability of the dopant: the formation energy of N dopants is less than half that of B dopants.

Note that none of the dopants cause magnetic moments to appear, although the total number of electrons per cell is odd. In accordance with previous calculations and experiment [14, 29], we can therefore conclude that the influence of the dopants is mainly restricted to charge doping (i.e. a shift of the Fermi level). This is nicely illustrated by the electronic band structure of the different systems, shown in figure 2. The graphene band structure is easily recognized for both kinds of substitutions although some clear shifts in the Fermi level are present according to the donor/acceptor character of the dopant. Such shifts agree well with the predictions based on the Dirac-cone picture, namely $E_{\mathrm{F}} = \hbar v_{\mathrm{F}}(\pi n_e)^{1/2}$ where v_{F} is the Fermi velocity and n_e the electron/hole excess density (i.e. the number of dopants per unit area).

Table 2. The bond length between X = B, N, C and the nearest-neighbor C atom (d_{CX}) and between X and the adsorbed H atom (d_{HX}), the buckling height (d_{GX}), the surface reconstruction energy (E_{surf}), the chemisorption energy (E_{chem}), and the magnetic moment (μ) for single H adsorption on doped and pure graphene.

	B		N		C	
	4 × 4	6 × 6	4 × 4	6 × 6	4 × 4	6 × 6
d_{CX}	1.520	1.525	1.507	1.507	1.503	1.504
d_{HX}	1.271	1.272	1.044	1.045	1.133	1.133
d_{GX}	0.267	0.261	0.386	0.389	0.355	0.353
E_{surf}	0.284	0.265	1.014	1.054	0.972	0.968
E_{chem}	−1.852	−1.826	−0.687	−0.661	−1.098	−1.090
μ	0.0	0.0	0.0	0.0	1.0	1.0

Note: Distances are given in Å, energies in eV, and magnetic moments in μ_B. Note that in the rightmost column, X refers to a carbon atom (pristine graphene).

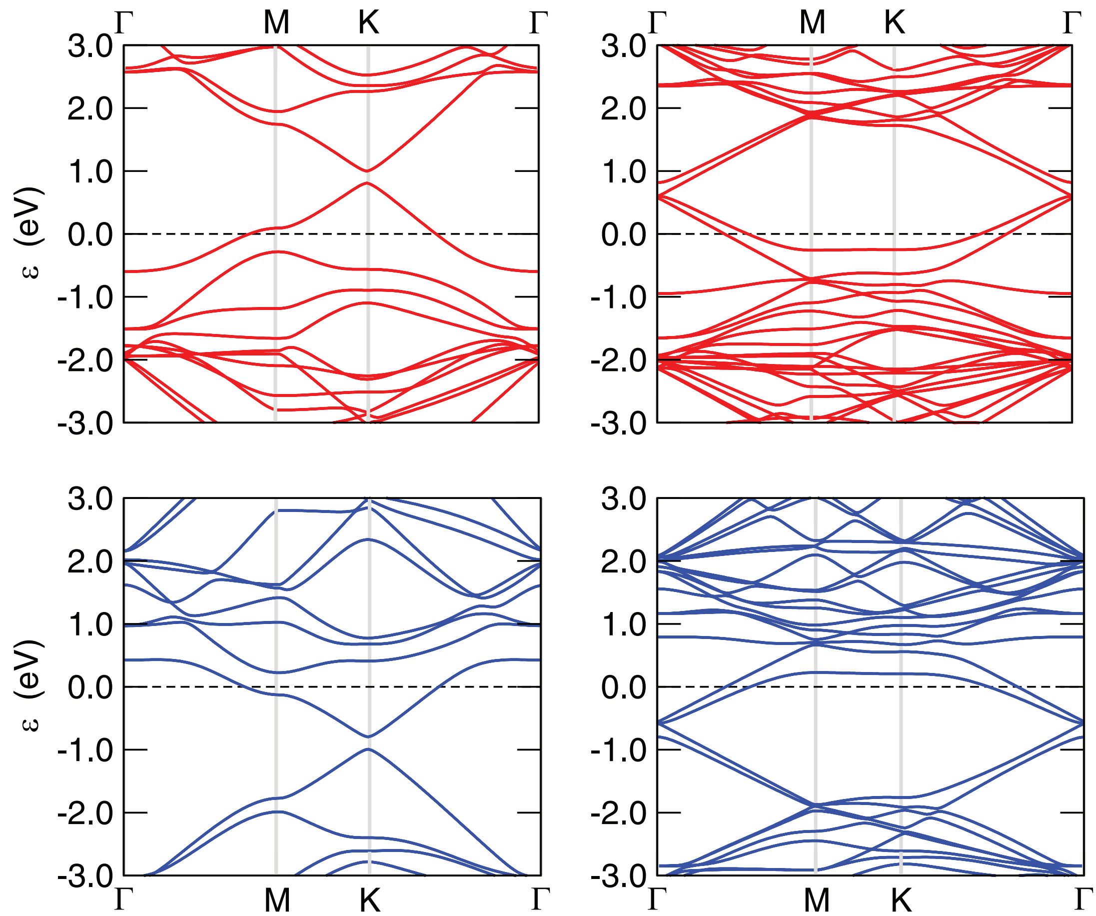

Figure 2. The electronic band structure of B-doped graphene (upper panels, in red) and N-doped graphene (lower panels, in blue) as obtained in a 4 × 4 (leftmost panels) and 6 × 6 (rightmost panels) supercells. The Fermi level is set to zero.

Closer inspection of the band structure around the Fermi level reveals some qualitative differences between the 4 × 4 and 6 × 6 supercells. While the B and N-doped 4 × 4 supercells exhibit semiconducting behavior, the 6 × 6 supercells are semimetallic. This is a consequence of the so-called 3N rule for the band structure of substitutionally doped graphene [31]. This rule states that $3N \times 3N$ supercells with a single substitution have a vanishing band gap, while the others exhibit semiconducting behavior, as simple symmetry arguments show [32, 33]. Note that these qualitative differences have only a minor influence of the stability and structural properties of the dopants, as discussed above.

3.2. Single H adsorption

3.2.1. Adsorption at the dopant site. Next, we consider the adsorption of H atoms on the substitutional defect atoms. The results for the two different supercells are given in table 2, along with those for single H adsorption on pure graphene, for comparative purposes. Note that the differences between the two supercells are again almost negligible, thereby suggesting that the results for the 6×6 cell are well-converged with respect to the supercell size.

Again, our findings are comparable to what can be found in the literature [18, 19, 34]. H adsorption induces a hybridization change from $sp^2$to sp^3 in the dopant atom and makes this atom bulge out of the graphene layer. We quantify this with the buckling height of the atom, which is defined as the difference in height between this atom and its three nearest neighbors, and with the surface reconstruction energy. There is a pronounced difference between the adsorption properties of B-doped, N-doped, and pure graphene. If we want to compare the chemisorption energies of the differently doped systems, we should take into account at least two different effects: (i) the internal stress of the initial and final state and (ii) the occupation of the bonding and anti-bonding orbitals (charge effect). Considering the approximate symmetric nature of the DOS around the Fermi level in graphene, we can assume that the effect of populating anti-bonding orbitals above the Dirac point or depopulating bonding orbitals below the Dirac point is similar. This can be grasped, for instance, by the magnitude of the Fermi level shifts which in both cases is ~0.5 eV for the concentrations of dopants considered here. In this way, chemisorption on B and N atoms should be comparable. The changes in the stress, on the other hand, are roughly similar only for H adsorption on N and C. This can be deduced from the similar changes in the C-X bond lengths, d_{CX}, the buckling height, d_{GX}, and the surface reconstruction energy, E_{surf}, shown in tables 1 and 2. In contrast, B-doped graphene presents a smaller change of the d_{CX} bond lengths upon hydrogenation, hence a much smaller E_{surf}. This strain effect (the difference between B and N) is much larger than the charge effect (the difference between C and N). In other words, the intrinsic strain of the B atom in the graphene lattice is reduced by the H adsorption. This leads to the relative order: $E_{\mathrm{chem}}(\mathrm{B}) < E_{\mathrm{chem}}(\mathrm{C}) < E_{\mathrm{chem}}(\mathrm{N})$. Summarizing, the opposite reactivity of B and N substitutions in graphene with a hydrogen atom is mainly governed by *surface relaxation* effects rather than charge effects, at variance with the conclusions of the authors of [19].

The chemisorption energies of the H atoms adsorbed on a C atom in pure graphene are in between those of H adsorption on B and N-doped graphene, but the magnetic properties are very different. In contrast to hydrogenation of pure graphene, the H atom does not induce any magnetism in the doped systems. Although this might be expected because of the even number of electrons per cell in the system, it is somewhat surprising because the substitutionally B and N-doped graphene does not show any magnetization either (see table 1). We discuss this finding in more detail below. These results can also be contrasted to B and N doping in fully hydrogenated graphene, i.e. graphane. In the last case N doping does not change the magnetic properties but B doping does [35].

3.2.2. Adsorption near the dopant site. The investigation of H adsorption on substitutionally doped graphene was not restricted to the defect site. It is an interesting question whether the H atom will actually prefer to adsorb at the dopant site, or rather in its neighborhood or as far as possible from the impurity. To investigate this, we consider the adsorption of a single H atom at various distances from the defect site in a 6×6 supercell (figure 3(a)). The chemisorption of the H atom is observed to become less favorable as the distance from the substitutional atom increases. This is true for both the B and the N dopant and might come as a surprise in the last case because adsorption at the N site is rather unfavorable. In fact, the most favorable adsorption site is the nearest-neighbor position w.r.t. the dopant site for both types of foreign atoms. At this site, the chemisorption energy is -2.22 and -2.01 eV for B and N-doped graphene respectively, which is about twice as large than on pure graphene. From the small wiggles of E_{chem} w.r.t. the distance (figure 3, upper inset), one can also observe a slight preference for adsorption at the other sublattice, i.e. at the *B* sublattice if the dopant is at the *A* sublattice. These results can be explained by the charge doping caused by the dopant atoms. Charge doping weakens the π bonds in graphene: electron doping leads to occupation of the anti-bonding π^* bands and hole doping decreases the population of the bonding π bands [36, 37]. Therefore, charge doping reduces the energy to break the π-bond network and enhances the stability of H chemisorption. The local charge doping of the B and N atoms strongly decreases with increasing distance to the dopant (see figures 3(b) and 4) and, consequently, the stability of the H atom decreases with the distance from the dopant site. In general, the H atom prefers adsorbing close the B atom rather than near the N atom. This small preference is due to the slightly larger sizes of the charges on the C atoms near a B dopant—a 'local' charge effect according to the analysis of [37]—and a slightly larger reactivity (towards hydrogen) of hole doped with respect to electron doped graphene [36] (see below the discussion on physical doping).

In order to illustrate the effect of the impurities on the charge density distribution ρ, we show in figure 4 the difference in ρ between hydrogenated doped graphene (with H chemisorbed at the most stable site, i.e. at the lattice position closest to the dopant) and pristine graphene. Two different effects can be identified. First, the effect of the substitutional atom, that leads to a high charge concentration at the dopant site and in its neighborhood: according to the electron-deficient (electron-rich) nature of the boron (nitrogen) atom, positive (negative) charge density is observed. Second, the effect of the hydrogen adatom which can be noticed from the reduced charge density at the sublattice on which H is adsorbed[4]. This break in the sublattice symmetry upon H adsorption is typical of π-conjugated systems and usually leads to a *spin* alternation [11]. In our case, the alternation shows up in the *charge* rather than in the spin density.

The substitutional doping has also a strong effect on the magnetic properties: due to the presence of B and N dopants, single hydrogen adsorption can not alter the magnetism of the system. This can be understood from the position of the defect levels induced by chemisorbed H atoms on graphene, as shown in figure 5. In pure graphene, the H atom leads to a

[4] This is best appreciated by looking at the differences in ρ between hydrogenated doped graphene and doped rather than pristine graphene (here not shown).

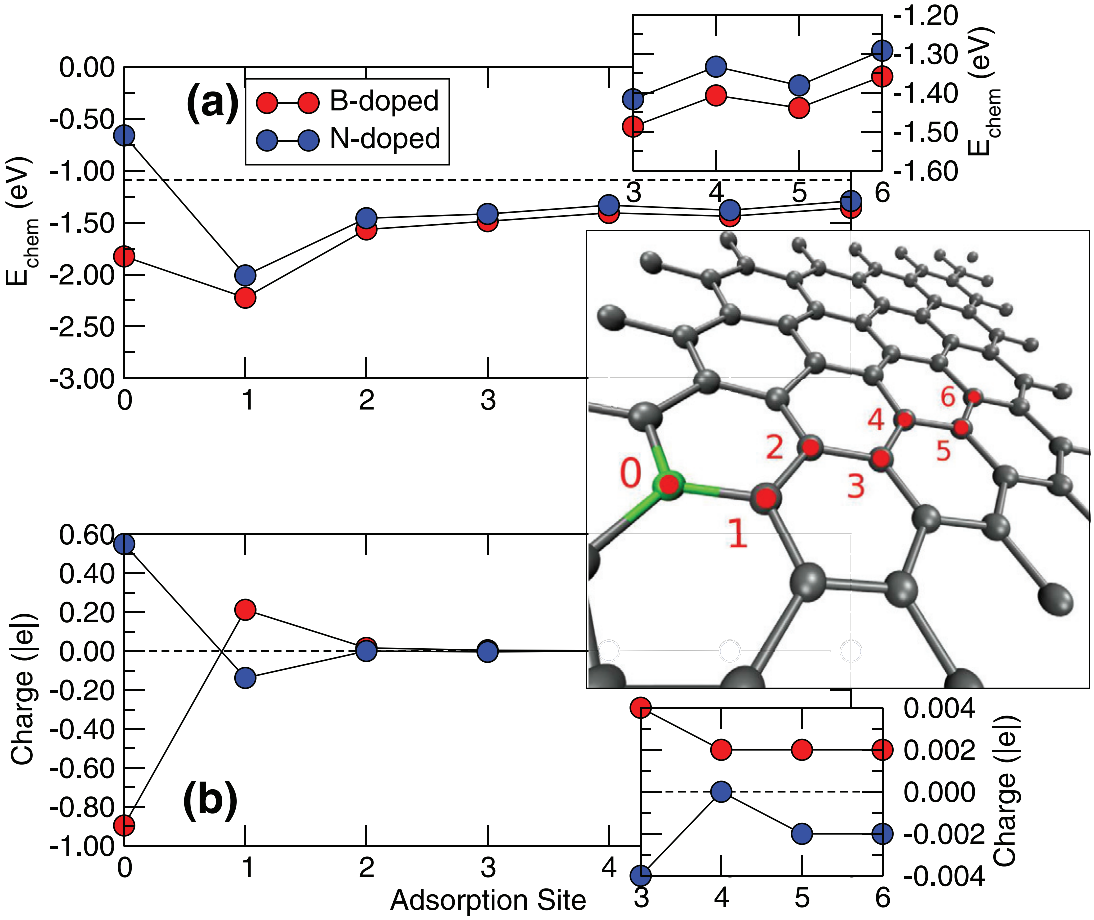

Figure 3. (a) The hydrogen chemisorption energy as a function of the adsorption site. The dashed line represents the chemisorption energy of a single H atom on pure graphene. (b) The Mulliken charges of the atoms at the adsorption sites in non-hydrogenated doped graphene. The middle inset shows the different adsorption sites, and the upper and bottom inset are close-ups of the far region for the chemisorption energies and Mulliken populations, respectively.

defect level at the Fermi level. This level is split in a spin-up and a spin-down level of which one lies above and the other below the Fermi level, inducing a magnetic moment of 1 μ_B in the system. In B-doped graphene, the Fermi level is lowered so that the H defect level is no longer occupied, while in N-doped graphene the Fermi level lies higher so that both (spin-up and spin-down) H levels are occupied. Therefore no change in the magnetization is observed, at least as long as the hydrogen concentration does not exceed the one of the dopant.

3.2.3. Physical doping. To gain further insight into the effects that the excess charges have on the reactivity of graphene, we broaden our investigation by considering ‘physical’ doping, as is typically realized by capacitatively coupling the carbon sheet to a gate electrode. In modeling this physical situation we used a graphene 4 × 4 supercell, and added variable amounts of charge in the range $[-1, +1]\,|e|$, always compensating it with a uniform background along the direction of the slab (but not in the vacuum region). The chosen size of the supercell allows a direct comparison with the B- and N-doped situations considered above, and the amount of excess charge covers the whole range of experimentally accessible carrier densities n_e. In fact, a charge $\pm|e|$ in a 4 × 4 supercell amounts to $\sim\pm3.125 \times 10^{-2}|e|$ per carbon atom (i.e. a carrier density of 1.69×10^{14} cm^{-2}) and, for a typical configuration with a 300 nm-thick SiO_2 insulating layer in between the graphene sheet and the gate electrode, this corresponds to a gate potential V_g of ±2340 V, well beyond the values typically used in practice (of course, smaller values of V_g would result when employing higher-κ dieletrics).

As discussed above, charge doping shifts the position of the Fermi level according to $\propto \sqrt{n}$ (figure 6, panel (a)), thus (de) populating the (π) π^* states and weakening the carbon-carbon bonds. This is evident from figure 6(b) where the cohesive energy of the lattice is seen to be *linearly* decreasing as a function of the excess charge. As a result, binding of a hydrogen atom is made easier by charge doping because of both (direct) electronic and (indirect) relaxation effects, and the H binding energy is found to increase (in an approximately quadratic way) with the charge density (figure 6(c)), with a slight preference for hole doping with respect to electron doping, similarly to what has been shown above for B- and N- doping, and in agreement with previous findings [36]. Contrary to substitutional doping, though, external charges spread out over the whole lattice, and have thus a weaker and uniform impact on its chemical properties. In fact, in the case of substitutional doping considered above, the ionized impurities create potential inhomogeneities and introduce distance-dependent effects

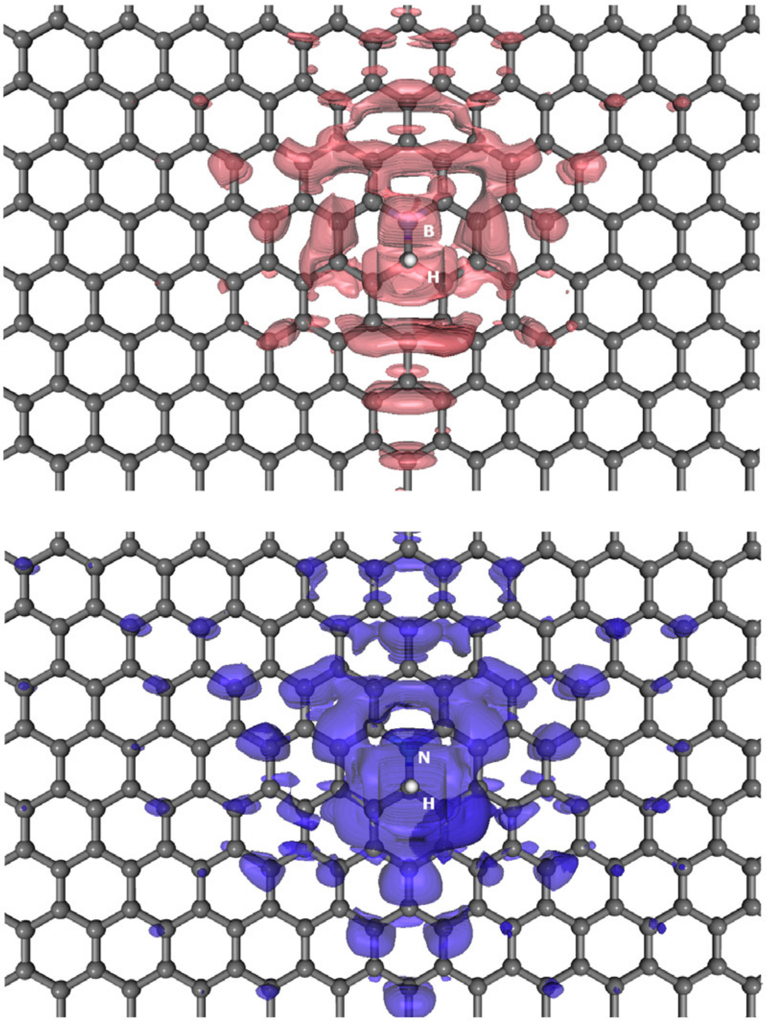

Figure 4. Difference in charge density between hydrogenated B-doped (upper panel) and N-doped (lower panel) graphene and pristine graphene, with isocontours at $\pm 0.0005\,|e|\,\mathring{A}^{-3}$. Hydrogen (white balls) is adsorbed at a C atom next to the dopant (red and blue balls for B and N, respectively). Red (blue) cloud represents positive (negative) charge density differences.

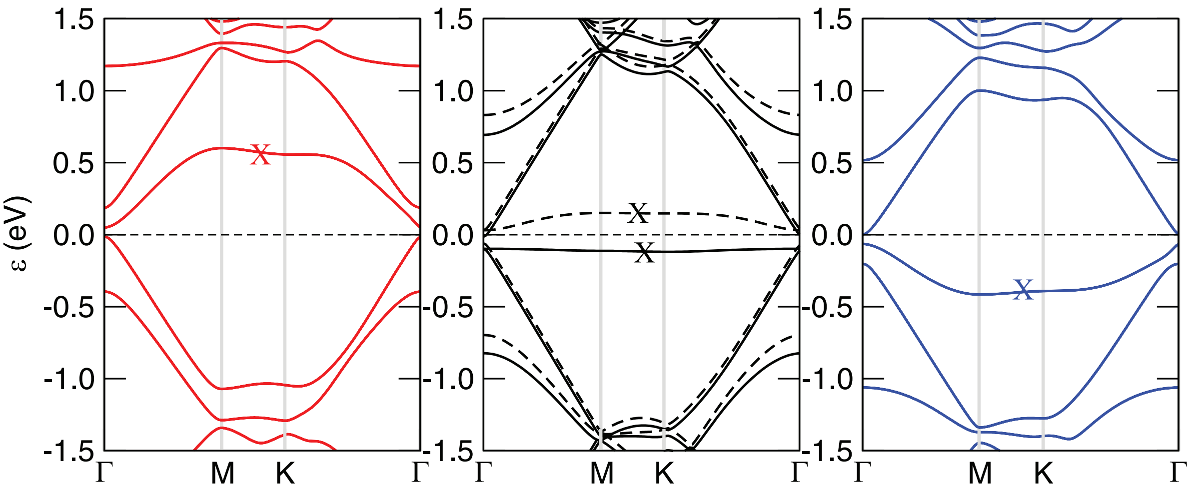

Figure 5. Electronic band structure upon H adsorption for B-doped (leftmost panel), pristine (center panel) and N-doped graphene (rightmost panel). For pristine graphene, solid (dashed) black lines indicate spin-up (spin-down) bands. Fermi level is set to zero. Crosses mark the defect-induced bands.

on the chemical properties (besides acting as strong, in-plane Coloumb scatterers for electrons). Overall, the hydrogen chemisorption energies reported in figure 3 compare well with those reported in figure 6(c), apart for the lattice positions closest to the dopant where binding is more favoured than expected on the basis of the (average) excess charge only.

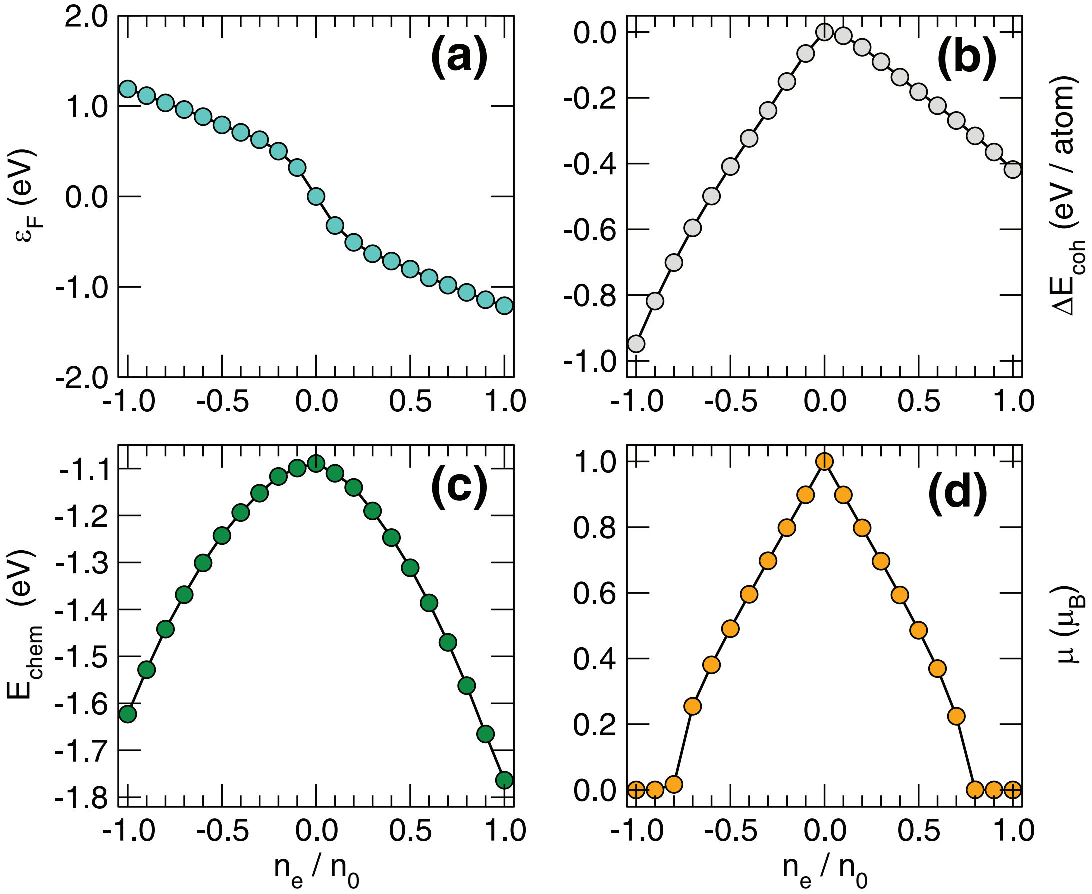

Figure 6. Energetic and magnetic properties as functions of the excess charge density n_e when physically doping the graphene sheet. In each panel but (b) n_e is given units of $n_0 = 1.69 \times 10^{14}$ cm^{-2}, corresponding to 1 $|e|$ in a 4×4 supercell; in (b) n_e is sixteen times larger. (a) Fermi level shift. (b) Difference in the cohesive energy between doped and charge-neutral graphene. (c) Hydrogen binding energy. (d) Magnetization of hydrogenated graphene (1 H atom in a 4×4 supercell).

Finally, the shift of the Fermi level induced by the introduction of holes or electrons in the system has a deep influence on the magnetic properties of the hydrogenated graphene. In the case of B or N substitutions, each dopant adds or removes one electron from the flake, and the magnetic moment accompanying H sticking gets completely quenched ($\mu = 0\,\mu_B$) as long as the hydrogen coverage does not exceed the dopant concentration, as discussed in the previous paragraph. Figure 6(d) shows that the same holds when physically doping the graphene sheet, and that the quenching of the magnetization is linear in n_e (as expected) and is already complete at $n_e \approx \pm 0.8$ n_H, where n_H is the surface density of hydrogen adatoms. This prediction could be experimentally tested by measuring the paramegnetic response of (weakly) hydrogenated graphene, which is expected to present a spin-half response sensitive to charge doping, as already shown to occur for the π-moment of the carbon atom vacancies when charge doping is provided by molecular adsorption [38].

3.3. H pair adsorption

As a final subject of investigation, we examine the adsorption process of H pairs. We use the most stable position for the first H atom on substitutionally doped graphene, i.e. at the nearest-neighbor site, and add a second H atom at various positions in a hexagonal ring that includes the dopant and the first adsorbed H atom (see figure 7). Because there are now two H atoms, there is the additional possibility of putting them on the same or opposite sides of the doped graphene layer. In practice, the possibility of realizing double- (as opposed to single-) sided hydrogenation depends on the experimental conditions, e.g. the presence of a substrate supporting the graphene sheet and of extendend defects/edges which typically

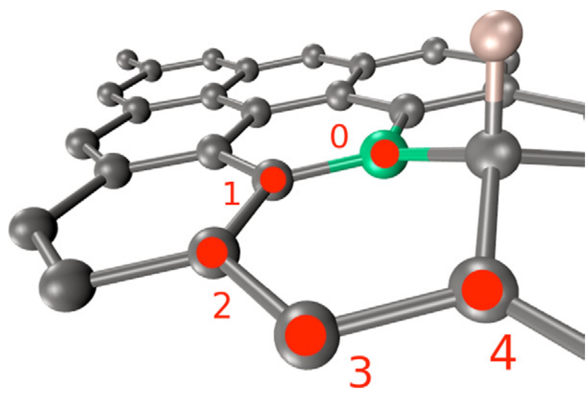

Figure 7. The investigated adsorption sites for the second H atom. The dopant atom is located at site 0.

Table 3. The chemisorption energy of the second H atom (E_{chem}), the total chemisorption energy ($E_{\text{chem}}^{\text{tot}}$) and magnetic moments ($\mu$).

	B			N		
	E_{chem}	$E_{\text{chem}}^{\text{tot}}$	μ	E_{chem}	$E_{\text{chem}}^{\text{tot}}$	μ
Site 0	−1.347	−3.590	0.0	−0.361	−2.399	0.0
Site 1	−1.574	−3.817	1.0	−1.485	−3.523	1.0
Site 2	−1.348	−3.591	0.0	−1.431	−3.469	0.0
Site 3	−1.143	−3.386	1.0	−1.084	−3.122	1.0
Site 4	−1.666	−3.909	0.0	−1.697	−3.735	0.0
Site $\bar{0}$	−1.731	−3.974	0.0	−1.152	−3.158	0.0
Site $\bar{1}$	−1.629	−3.872	1.0	−1.452	−3.490	1.0
Site $\bar{2}$	−1.208	−3.451	0.0	−1.310	−3.348	0.0
Site $\bar{3}$	−1.037	−3.280	1.0	−1.130	−3.168	1.0
Site $\bar{4}$	−2.100	−4.343	0.0	−2.303	−4.341	0.0

Note: Energies are given in eV and magnetic moments in μ_B. A bar over the number of the adsorption site means chemisorption at the opposite side.

allow H atoms to reach the substrate and diffuse in between the cabon sheet and the support. The chemisorption energies of the second H atom and the resulting magnetic moment of the total system are reported in table 3. They were obtained using the 4×4 graphene supercell because we only considered adsorption close to the dopant. The results agree well with the findings of some previous partial studies of the subject [17, 18, 20, 39].

Double-sided chemisorption is strongly preferred over adsorption on the same side for neighboring adsorption sites (sites 0 and 4). When the second H atom is chemisorbed farther away from the first one (sites 1–3) the chemisorption energies are not very different and single-sided adsorption can become more favorable. This finding is very similar to what has been observed for H pair adsorption on pure graphene [11, 34], indicating that this is mainly a structural effect. In fact, one can expect the presence of two competing effects. First there is the charge doping that favors adsorption sites near the dopant (site 1), and second, there is a structural effect that favors adsorption next to the first H atom (sites 0 and 4) as in pure graphene. This structural effect is present for both single and double-sided adsorption, but is stronger for the double-sided case. The stability of the different H configurations follows from these two competing effects and leads to the relative stability sequence $E_{\text{chem}}(4) < E_{\text{chem}}(1) < E_{\text{chem}}(2) < E_{\text{chem}}(3)$ for both single and double-sided adsorption. The chemisorption energy at the dopant site, $E_{\text{chem}}(0)$, forms a special case because it is very different for B and N dopants as discussed above. The most stable H configurations are those with the second H atom adsorbed on a C atom neighboring the site where the first H is adsorbed (i.e. the *ortho* site). Contrary to the adsorption of a single H atom, the chemisorption of a second H atom can be more stable on N-doped graphene as compared to B-doped graphene. The total chemisorption energy of H pairs presents therefore more similar values for B and N-doped graphene, though a larger stability (0.0–0.3 eV) of the B-doped case remains. The most stable H pair configuration has a total chemisorption energy of −4.34 eV for both dopants. This can be compared with the chemisorption energy for a H pair on pure graphene which is −2.81 eV. H pair adsorption is therefore more stable on doped graphene than on pure graphene. Energies for sequential adsorption are larger than the hydrogen binding energy far from the dopant site (see e.g. the single-sided chemisorption energies reported in table 3), thereby suggesting that clustering is likely to occur close to a B- or N-dopant atom. Doping with B or N species does suppress dimer and cluster formation through competitive binding to the site closest to the dopant (the above energies are smaller than the H–binding energies to the sites nearest to the dopant), but only as long as some dopant species is available for sequestrating hydrogen atoms. For larger H coverages the formation of dimers *close* to the dopant sites is energetically preferred over hydrogenation of the pristine graphene sheet, hence clustering is expected to be *more likely* close to B or N atoms than in the clean areas of the graphene surface. This finding contradicts the conclusion of [18].

Also shown in Table 3 is the magnetic moment of the different configurations considered. Some of the H pair configurations produce a magnetic moment of 1 μ_B. The magnetic moment is always the same for single and double-sided adsorption, so it only depends on the adsorption site. If the two H atoms are chemisorbed on the same graphene sublattice the magnetic moment is 1 μ_B, and it vanishes when the H atoms are adsorbed at different sublattices. This can be compared to H pair adsorption on pure graphene. In the last case the magnetic moment is always 0 or 2 μ_B, depending on whether the two H atoms are chemisorbed on different or the same sublattice, respectively [11, 34, 40]. So the influence of the B or N dopant is to reduce the magnetic moment from 2 to 1 μ_B for adsorption at the same sublattice, while it does not change the magnetic properties in the other case. The last case is easy to understand since B or N doping does not change the magnetic properties of non-magnetic systems because it only shifts the Fermi level, as discussed above. The case of the same-sublattice adsorption can be understood in a similar way: without the dopant the magnetic moment would be 2 μ_B, but the Fermi-level shift induced by the dopant removes 1 μ_B by adding (removing) one electron to (from) the spin-split defect levels above (below) the Fermi-level in the case of N (B) doping (see figure 8). Population analysis reveals that the unpaired electron is mainly located on the sublattice where no H atoms are adsorbed and in the neighborhood of these H atoms. This is comparable to what happens in pure graphene, although there is only one unpaired electron in the doped case. Another difference is the reduction of the spin density at and near the dopant site.

4. Summary and conclusions

In this work we presented a first-principles investigation of atomic hydrogen chemisorption on boron and nitrogen doped graphene.

We demonstrated that the substitutional doping does not induce magnetism and that its main influence is restricted to charge doping.

First we focused on single hydrogen chemisorption: we considered the hydrogenation both on the substitutional foreign atom and on the carbon atoms near the dopant. We

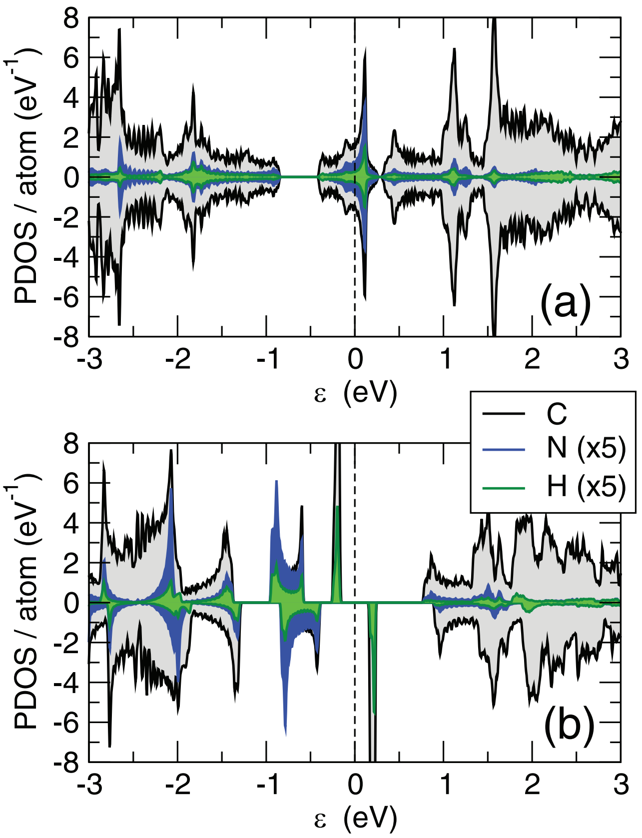

Figure 8. The PDOS of N-doped graphene for H pair adsorption at sites 1 (i.e. Hs in *meta* positions, panel (a)) and 4 (i.e. Hs in *ortho* position, panel (b)). The DOS projected on the carbon atoms are averaged over the lattice sites in the supercell and the Fermi-level is set to zero.

observed that hydrogenation of boron (nitrogen) is more (less) favorable than the hydrogenation of pure graphene. We also evaluated the chemisorption energy as a function of the distance from the defect, up to about 7.5 Å and found out that the presence of a dopant atom stabilizes the adsorbed H atom. This observation was shown to be caused by the charge doping of the dopant atoms, that leads to a preferential adsorption of hydrogen on the C atom closest to the defect, with a chemisorption energy that is about twice as large as on pristine graphene. This effect is independent of the nature of the foreign atom, and shown to occur also when physically doping the graphene sheet, e.g. by electrostatic gating. Furthermore, the hydrogenation becomes less stable as the distance from the defect increases because the net charge on the C atoms diminishes. Contrary to the case of single hydrogenation of graphene, no magnetic moment was found in doped graphene.

We also considered H pair adsorption. We investigated the most stable structures of both single and double-sided adsorption close to the dopant. We found out that the second H atom prefers to chemisorb on the *ortho* site (i.e. next to the other adsorbed H atom) on the opposite side of the layer, since this configuration minimizes the structural distortion. In general, the chemisorption energy of the H pair is determined by three competing effects, charge doping, sublattice alternation and structural effects. Clearly, only the latter two show up in pristine, charge-neutral graphene. In doped graphene charge doping does play a role and changes the relative stability of the doubly hydrogenated configurations, making some *meta* (magnetic) configurations—namely, those with both H atoms next to the dopant—very stable. In general, and similarly to undoped graphene, magnetic configurations always result when two H adsorb on the same sublattice. Contrary to graphene, a magnetization equal to 1 μ_B was observed in doped graphene, as a consequence of charge doping that partially quenches the magnetic moment. The projected density of states together with a population analysis revealed that the unpaired electron is delocalized on *ortho* and *para* sites w.r.t. the hydrogenated carbon atoms.

In conclusion, one can say that boron and nitrogen substitutions have a similar effect on single-H and H-pair adsorption, although they lead to opposite charge doping and different structural effects in graphene. They both quench the magnetism related to the hydrogen-induced π moments, thereby suggesting that the paramagnetic response of hydrogenated B-doped (N-doped) graphene is sensitive to negative (positive) charges injected into the system. Finally, both B- and N- dopants favor dimer formation and clustering in their neighborhoods, and this suggests that selective hydrogenation is possible in B- or N-rich areas of graphene.

Acknowledgments

This work was supported by the Flemish Science Foundation (FWO-Vl). MP gratefully acknowledges the Condensed Matter Theory group at Universiteit Antwerpen for the hospitality during his stay.

References

[1] Novoselov K S, Geim A K, Morozov S V, Jiang D, Zhang Y, Dubonos S V, Grigorieva I V and Firsov A A 2004 *Science* **306** 666
[2] Novoselov K S, Jiang D, Schedin F, Booth T J, Khotkevich V V, Morozov S V and Geim A K 2005 *Proc. Natl Acad. Sci. USA* **102** 10451
[3] Elias D C *et al* 2009 *Science* **323** 610
[4] Bostwick A, McChesney J L, Emtsev K V, Seyller T, Horn K, Kevan S D and Rotenberg E 2009 *Phys. Rev. Lett.* **103** 056404
[5] Balog R *et al* 2010 *Nat. Mater.* **9** 315
[6] Ströbel R, Garche J, Moseley P, Jörissen L and Wolf G 2006 *J. Power Sources* **159** 781
[7] Assfour B, Leoni S, Seifert G and Baburin I A 2011 *Adv. Mater.* **23** 1237
[8] Chambers A, Park C, Baker R T K and Rodriguez N M 1998 *J. Phys. Chem.* B **102** 4253
[9] Bonaccorso F, Colombo L, Yu G, Stoller M, Tozzini V, Ferrari A C, Ruoff R S and Pellegrini V 2015 *Science* **347** 6217
[10] Peres N M R 2010 *Rev. Mod. Phys.* **82** 2673
[11] Casolo S, Løvvik O M, Martinazzo R and Tantardini G F 2009 *J. Chem. Phys.* **130** 054704
[12] Panchakarla L S, Subrahmanyam K S, Saha S K, Govindaraj A, Krishnamurthy H R, Waghmare U V and Rao C N R 2009 *Adv. Mater.* **21** 4726
[13] Zhao L *et al* 2011 *Science* **333** 999
[14] Liu H, Liu Y and Zhu D 2011 *J. Mater. Chem.* **21** 3335

[15] Ekimov E A, Sidorov V A, Bauer E D, Mel'nik N N, Curro N J, Thompson J D and Stishov S M 2004 *Nature* **428** 542
[16] Savini G, Ferrari A C and Giustino F 2010 *Phys. Rev. Lett.* **105** 037002
[17] Zhu Z H, Lu G Q and Hatori H 2006 *J. Phys. Chem.* B **110** 1249
[18] Miwa R H, Martins T B and Fazzio A 2008 *Nanotechnology* **19** 155708
[19] Zhou Y G, Zu X T, Gao F, Nie J L and Xiao H Y 2009 *J. Appl. Phys.* **105** 014309
[20] Zhu Z H, Hatori H, Wang S B and Lu G Q 2005 *J. Phys. Chem.* B **109** 16744
[21] Hohenberg P and Kohn W 1964 *Phys. Rev.* **136** B864
[22] Kohn W and Sham L J 1965 *Phys. Rev.* **140** A1133
[23] Soler J M, Artacho E, Gale J D, García A, Junquera J, Ordejón P and Sánchez-Portal D 2002 *J. Phys.: Condens. Matter* **14** 2745
[24] Perdew J P, Burke K and Ernzerhof M 1996 *Phys. Rev. Lett.* **77** 3865
[25] Troullier N and Martins J L 1991 *Phys. Rev.* B **43** 1993
[26] Monkhorst H J and Pack J D 1976 *Phys. Rev.* B **13** 5188
[27] Wu M, Cao C and Jiang J Z 2010 *Nanotechnology* **21** 505202
[28] Rani P and Jindal V K 2013 *RSC Adv.* **3** 802
[29] Leenaerts O, Sahin H, Partoens B and Peeters F M 2013 *Phys. Rev.* B **88** 035434
[30] Lazar P, Zboril R, Pumera M and Otyepka M 2014 *Phys. Chem. Chem. Phys.* **16** 14231
[31] Zhou Y-C, Zhang H-L and Deng W-Q 2013 *Nanotechnology* **24** 225705
[32] Casolo S, Martinazzo R and Tantardini G F 2011 *J. Phys. Chem.* C **115** 3250
[33] Martinazzo R, Casolo S and Tantardini G F 2010 *Phys. Rev.* B **81** 245420
[34] Boukhvalov D W, Katsnelson M I and Lichtenstein A I 2008 *Phys. Rev.* B **77** 035427
[35] Wang Y, Ding Y, Shi S and Tang W 2011 *Appl. Phys. Lett.* **98** 163104
[36] Huang L F, Ni M Y, Zhang G R, Zhou W H, Li Y G, Zheng X H and Zeng Z 2011 *J. Chem. Phys.* **135** 064705
[37] Gong P L, Huang L F, Zheng X H, Zhang Y S and Zeng Z 2015 *J. Phys. Chem.* C **119** 10513
[38] Nair R R, Tsai I-L, Sepioni M, Lehtinen O, Keinonen J, Krasheninnikov A V, Neto A H C, Katsnelson M I, Geim A K and Grigorieva I V 2013 *Nat. Commun.* **4** 2010
[39] Ferro Y, Marinelli F, Allouche A and Brosset C 2003 *J. Chem. Phys.* **118** 5650
[40] Ferro Y, Teillet-Billy D, Rougeau N, Sidis V, Morisset S and Allouche A 2008 *Phys. Rev.* B **78** 085417